Asian Engineering Review
Vol. 13, No. 1, 26-34, 2026
ISSN(E) 2409-6725/ ISSN(P) 2518-0150
DOI: 10.20448/aer.v13i1.8829

Artificial intelligence–driven optimal control and bifurcation avoidance in semiconductor laser systems

Lakshmi N Sridhar

Chemical Engineering Department, University of Puerto Rico, Mayaguez, Puerto Rico.
Email: lakshmin.sridhar@upr.edu

Abstract

Injection-locked semiconductor lasers feature a complex nonlinear dynamic response due to the coupling between the carrier density and optical field in the presence of an external driving force. Although this class of systems has been used to achieve many interesting photonic capabilities, they are quite unstable and prone to Hopf bifurcations, leading to self-oscillations that undermine their effectiveness in applications where stable operation is critical. In this study, a full computational framework is constructed to investigate and control the dynamics of injection-locked semiconductor lasers. A dimensionless system is established using coupled rate equations to describe the physical processes within it. The stability boundaries and Hopf bifurcations are determined by performing bifurcation analysis using the MATCONT software package. To incorporate stability constraints into the optimization algorithm, a neural network surrogate is developed to predict the maximum real part of the system's eigenvalues as a function of both state variables and control parameters. A soft penalty-based method is used to avoid operation close to an unstable region, thus imposing stability without any non-smooth restrictions on the system. The corresponding optimization problem is solved by employing IPOPT. It is shown that the developed method suppresses oscillatory behavior, producing smoother control inputs with better objective function performance than no control at all. This combination of techniques yields a versatile numerical scheme for stabilization of nonlinear photonic systems, which can be applied to a large variety of systems with instability caused by bifurcations.

Keywords: Artificial intelligence, Bifurcation analysis, Nonlinear dynamical systems, Optimal control, Stability-constrained optimization.

Citation | Sridhar, L. N. (2026). Artificial intelligence–driven optimal control and bifurcation avoidance in semiconductor laser systems. *Asian Engineering Review*, *13*(1), 26–34. 10.20448/aer.v13i1.8829
History:
Received: 27 April 2026
Revised: 29 May 2026
Accepted: 15 June 2026
Published: 18 June 2026

Publisher: Asian Online Journal Publishing Group

Funding: This study received no specific financial support.
Institutional Review Board Statement: Not applicable.
Transparency: The author confirms that the manuscript is an honest, accurate, and transparent account of the study; that no vital features of the study have been omitted; and that any discrepancies from the study as planned have been explained. This study followed all ethical practices during writing.
Competing Interests: The author declares that there are no conflicts of interest regarding the publication of this paper.

Contents

Contribution of this paper to the literature
The main contribution of this paper is the development of an integrated framework combining bifurcation analysis and optimal control for semiconductor laser systems. The study links nonlinear dynamical behavior, stability transitions, and control design, enabling the suppression of oscillatory laser dynamics, providing insight into parameter-dependent instabilities and performance optimization.

1. Introduction

Semiconductor lasers play an important role in contemporary photonic devices across various fields, including optics, communications, sensing, and neuromorphic computing. Among the types of semiconductor lasers, injection-locked semiconductor lasers are of particular interest for their ability to exhibit improved characteristics and various types of nonlinear dynamics under the influence of external optical driving. The interaction between the optical field and the carrier population in a slave laser due to coherent injection from a master laser gives rise to different dynamics, including steady-state locking, periodic and quasi-periodic oscillations, and even chaotic oscillations.

An important feature of these models is bifurcation, specifically Hopf bifurcation, which marks the point at which oscillations emerge from what would otherwise be a stable fixed point. Although this feature might be advantageous in some cases, the instability it introduces is generally undesirable in practical situations where the laser must operate steadily and reliably. Thus, avoiding bifurcations is crucial in obtaining reliable results. To do this, we need tools such as numerical continuation provided by MATCONT to model these nonlinear dynamical systems. However, directly embedding bifurcation calculations into optimization and control frameworks remains computationally challenging.

A methodology is introduced that combines bifurcation analysis, machine learning techniques, and optimal control methods to stabilize unwanted oscillations of injection-locked semiconductor lasers. First, the model is non-dimensionalized, and bifurcations are analyzed using MATCONT to identify Hopf bifurcations and stability domains. To efficiently incorporate stability constraints into the control problem, a neural network estimates the boundary of the stability domain. The neural network model is integrated within a Pyomo optimal control design with penalty functions. This scheme offers an effective approach for managing nonlinear dynamical systems subject to stability constraints.

2. Literature Review

Dynamical analysis of semiconductor lasers has received significant attention from the research community over the past few decades, beginning with the pioneering work of Robert Lang, who identified the characteristics of injection locking of semiconductor lasers and proposed a model describing the interaction between the injected optical field and the laser's dynamic response [1]. Subsequent advancements in semiconductor laser theory, including works by authors such as Agrawal and Dutta [2] and Coldren, et al. [3] provided a comprehensive physical understanding of carrier-photon interactions through rate equations.

The incorporation of optical injection and feedback results in a range of interesting nonlinear dynamical properties, including multistability, self-pulsations, and chaos. These have been studied systematically using dynamical systems theory with notable works by Krauskopf and Wieczorek [4] and Wieczorek, et al. [5] where they highlighted the complexity of bifurcations in optically injected semiconductor lasers and pointed out the significance of Hopf, saddle-node, and global bifurcations. Delay effects and slow-fast dynamics were further emphasized by studies Erneux and Glorieux [6].

Research on nonlinear waves, such as phase solitons and domains, in semiconductor lasers was also considered an important topic due to its implications for understanding the system's spatial-temporal complexity. Experimental studies were conducted by Gustave, et al. [7] and theoretical studies by Garbin, et al. [8] to highlight phase solitons and the complex temporal dynamics coexisting with coherent structures in optically injected systems. Meanwhile, Terrien, et al. [9] explored delayed feedback models in semiconductor lasers, such as the Yamada model, demonstrating that delay-induced bifurcations can significantly alter system stability and lead to oscillatory regimes.

Recent innovations have focused on harnessing the capabilities of nonlinear dynamical systems that characterize the operation of semiconductor lasers to create useful devices. The investigations by Torre and Masoller [10] and Virte, et al. [11] have demonstrated that chaotic and nonlinear dynamical behavior can be used for sensing and communication tasks. Additionally, the rise of photonic and neuromorphic computing has made semiconductor lasers critical elements in future information processing paradigms. This is evident in works by Robertson, et al. [12]. Delayed and photonic reservoir computing was explored in works such as those by Soriano, et al. [13] and Mørk, et al. [14].

Other related works from 2022 to 2024 concern the manipulation and control of non-linear dynamism in injection-locked semiconductor lasers. Bifurcation control and dynamic regimes were examined in papers by Li, et al. [15] and Wang, et al. [16]. On the other hand, Liu, et al. [17] proposed optical activation functions based on injection-locked lasers, thus connecting nonlinear optics with artificial intelligence. More recent works by Heil, et al. [18], Zhang, et al. [19] and Shen, et al. [20] have shown the relevance of these devices for photonic neural networks and dynamic control.

On a more mathematical level, the investigation of the above system is highly dependent on the use of bifurcation theory and numerical continuation techniques. Fundamental works in the literature can be credited to authors such as Kuznetsov [21] and Govaerts [22], who provided the mathematical framework for investigating stability and bifurcations in nonlinear systems. Moreover, with the advent of numerical methods, such as MATCONT [23], the calculation of equilibrium curves, limit cycles, and Hopf bifurcations is now feasible for highly complicated laser models.

In summary, the literature has established that optically injected semiconductor lasers form a canonical example of nonlinear dynamical systems, applicable in physics and engineering systems. There is still room for

developing models that combine physical intuition and nonlinear dynamics without compromising any aspects. This paper aims to accomplish this by developing a nondimensionalized model that is both physically realistic and analyzable via bifurcations.

The primary goal of this study is to formulate and apply an optimal control approach for controlling an injection-locked semiconductor laser system, in which undesired oscillations are suppressed via a soft constraint that avoids Hopf bifurcation. This particular dynamical system is modeled using the rate equations formulated by Lang [1] that describe injection locking in semiconductor lasers, as well as those used in conventional semiconductor lasers [2, 3, 5]. The rate equation describes the nonlinear relationship between the carrier density and the optical field, which can give rise to Hopf bifurcations and hence oscillatory behavior. Bifurcation analysis is carried out using bifurcation theory and numerical continuation with MATCONT [23]. Based on this work, the computed stability boundaries are integrated into an optimal control problem framework, formulated to ensure the system operates well clear of Hopf bifurcations via a soft penalty approach. The optimal control problem can subsequently be formulated as an NLP and solved using advanced optimization algorithms in Pyomo [24] and the IPOPT solver [25]. In this way, this comprehensive framework facilitates the efficient computation of optimal operational policies that ensure steady-state laser operation in stable operating regions.

2.1. Injection-Locked Semiconductor Laser Model Equations

The injection-locked semiconductor laser is a system in which the slave laser is forced externally by a coherent optical field from the master laser. The master laser forces the coherent optical field into the slave laser's cavity. This phenomenon, known as optical injection locking, is an essential component of modern photonics and optoelectronics. When a coherent optical field is applied to the injection-locked semiconductor laser, it affects both the amplitude and the phase of the slave laser's output. Depending on various system parameters, the laser can either remain locked to the input signal and operate in the steady-state regime or display oscillations, quasi-periodicity, and even chaos. Various experiments and theories have confirmed that injection-locked semiconductor lasers exhibit interesting nonlinear phenomena, such as Hopf bifurcation and self-sustained oscillations. Nonlinear dynamics of injection-locked semiconductor lasers can be studied analytically by employing rate equations that model optical and carrier dynamics in a coupled fashion. Such dynamics describe the optical and carrier fields as a nonlinear dynamical system with multiple timescales. The dimensionless form of the injection-locked semiconductor laser model is written in terms of the real and imaginary parts of the optical field and the carrier density. An injection-locked semiconductor laser consists of a slave laser subject to coherent optical injection from a master laser. The injected field modifies both the amplitude and phase of the slave laser output, leading to a wide range of nonlinear dynamical behaviors including steady-state locking, oscillations, and bifurcations. These effects arise from the interaction between the carrier density and the optical field inside the semiconductor cavity under external forcing.

The dynamics of such systems are well described by coupled rate equations for the optical field and carrier density. These equations capture the essential physics of stimulated emission, carrier recombination, and optical injection, and have been widely used to study bifurcations and instabilities in semiconductor lasers. The dimensional model for an injection-locked semiconductor laser is given by:

$$\begin{aligned}
\frac{dN_{\dim}}{dt} &= \frac{I}{qV} - \frac{N_{\dim}}{\tau_n} - g_0(N_{\dim} - N_{tr})(E_x^2 + E_y^2) \\
\frac{dE_x}{dt} &= \left(\frac{1}{2}\right)(N_{dim} - N_{tr})E_x - \left(\frac{\alpha}{2}\right)(N_{dim} - N_{tr})E_y + \kappa E_{inj} \qquad (1) \\
\frac{dE_y}{dt} &= \left(\frac{1}{2}\right)(N_{dim} - N_{tr})E_y + \left(\frac{\alpha}{2}\right)(N_{dim} - N_{tr})E_x - \Delta E_x
\end{aligned}$$

N_{dim} is the Carrier density (m^{-3}); E_x, E_y, are the Electric field components; I is the injection current (A); q is the electron charge (C); V is the carrier lifetime (s); τ_p the photon lifetime (s); g_0 the differential gain (m^3/s); N_{tr} the transparency carrier density (m^{-3}); α the linewidth enhancement factor; κ the injection coupling coefficient; E_{inj} the injected the field amplitude and Δ, the frequency detuning. We assume $\tau_p = \tau_n$.

Defining dimensionless variables as $\tau = \frac{t}{\tau_p}; N = \frac{N_{\dim}}{N_{tr}}; E_0^2 = \frac{1}{g_0 N_{tr} \tau_p}; x = \frac{E_x}{E_0}; y = \frac{E_y}{E_0}; K = \frac{\kappa E_{inj}\ \tau_p}{E_0}$ we get

$$\begin{aligned}
\frac{dx}{d\tau} &= \frac{1}{2}(N-1)x - \frac{\alpha}{2}(N-1)y + K \\
\frac{dy}{d\tau} &= \frac{1}{2}(N-1)y + \frac{\alpha}{2}(N-1)x - \Delta x \qquad (2) \\
\frac{dN}{d\tau} &= \frac{\tau_p}{N_{tr}}\left(\frac{1}{qV}\right) - \frac{N\tau_p}{\tau_n} - (N-1)(x^2 + y^2)
\end{aligned}$$

Using $\tau_p = \tau_n$ and $P = \frac{\tau_p}{N_{tr}}\left(\frac{1}{qV}\right)$ (the pump parameter) third equation reduces to:

$$\frac{dN}{d\tau} = P - N - (N-1)(x^2 + y^2) \qquad (3)$$

To incorporate nonlinear gain saturation, we modify the stimulated emission term $(N-1)(x^2+y^2) \to (1+2N)(x^2+y^2)$.

The ultimate no-dimensional equation set would be:

$$\frac{dx}{d\tau} = \frac{1}{2}(N-1)x - \frac{\alpha}{2}(N-1)y + K$$

$$\frac{dy}{d\tau} = \frac{1}{2}(N-1)y + \frac{\alpha}{2}(N-1)x - \Delta x$$
$$\frac{dN}{d\tau} = P - N - (1+2N)(x^2+y^2) \quad (4)$$

These equations describe a three-dimensional nonlinear dynamical system modeling the interaction between the optical field and the carrier population. The variables in the model are defined as follows.

- x(t): Real part of the complex electric field (dimensionless).
- y(t): Imaginary part of the complex electric field (dimensionless).
- N(t): Carrier density (dimensionless, normalized with respect to the threshold value).

The complex optical field can be written as:

$$E(t) = x(t) + iy(t) \quad (5)$$

The physically measurable optical intensity is given by:

$$I(t) = x^2(t) + y^2(t) \quad (6)$$

Which is always non-negative and corresponds to the emitted laser power. The carrier density (N(t)) represents the excess population of charge carriers (electrons and holes) in the semiconductor active region. It evolves on a slower time scale compared to the optical field.

The parameters appearing in the model have clear physical interpretations:

- α : Linewidth enhancement factor (dimensionless). This parameter accounts for amplitude–phase coupling in semiconductor lasers and is typically within the range ($2 < \alpha < 5$).
- K: Injection strength (dimensionless). This parameter represents the amplitude of the optical field injected from the master laser into the slave laser cavity. Typical values are from 0.1 to 1.5.
- Δ : Frequency detuning (dimensionless). This represents the difference between the optical frequency of the master laser and that of the free-running slave laser. The values range from 1 to 5.
- P: Pump parameter (dimensionless). This represents the normalized injection current or pumping level of the semiconductor laser. Values of (P > 1) correspond to operation above the lasing threshold. The usual values are from 1.2 to 2.

The first two equations describe the evolution of the optical field due to gain, amplitude-phase coupling, and injection from another source. The last equation accounts for the evolution of the carrier population due to input pumping and stimulated emission losses. Feedback loops arising from the nonlinear interactions between the optical intensity and the carrier density can destabilize the steady state. For example, the feedback resulting from the combination of the injection field, detuning, and the carrier population leads to oscillatory instability through Hopf bifurcations. A Hopf bifurcation marks the onset of periodic oscillations in the laser's output, which are common in injection-locked semiconductor lasers. The injection-locked semiconductor laser under consideration is a three-dimensional nonlinear dynamical system. It includes amplitude-phase coupling, external injection, and nonlinear carrier dynamics, thereby exhibiting a range of behaviors, including steady-state operation, oscillations, and bifurcations. Such a system is a good candidate for the study of Hopf bifurcations.

2.2. Bifurcation Analysis and Optimal Control

2.2.1. Bifurcation Analysis

Bifurcation calculations are performed using the MATLAB software MATCONT. Bifurcation analysis explains the main causes of multiple steady states and limit cycles. Branch points and limit points cause multiple steady-state solutions, while limit cycles and oscillatory behavior are caused by Hopf bifurcation points. The MATLAB program that effectively locates limit points, branch points, and Hopf bifurcation points is MATCONT. This program was developed and improved by several researchers [23, 26]. This program is very effective in identifying limit points (LP), branch points (BP), and Hopf bifurcation points (H) for a system of ordinary differential equations.

$$\frac{dx}{dt} = f(x, \alpha) \quad (7)$$

$x \in R^n$ where the bifurcation parameter is α. The gradient vector is orthogonal to the tangent and hence the tangent plane at any point $w = [w_1, w_2, w_3, w_4, \ldots . w_{n+1}]$ must satisfy.

$$Aw = 0 \quad (8)$$

The matrix A is defined by.

$$A = [\partial f/\partial x \quad |\partial f/\partial \alpha] \quad (9)$$

The sub-matrix $\partial f/\partial x$ is the Jacobian matrix. For both limit and branch points, the Jacobian matrix $J = (\partial f/\partial x)$ must have a determinant of 0.

At a limit point, the $n+1^{th}$ component of the tangent vector $w_{n+1} = 0$. For a branch point, the matrix $B = \begin{bmatrix} A \\ w^T \end{bmatrix}$ must be singular and have a determinant of 0.

At a Hopf bifurcation point,

$$det(2f_x(x, \alpha) @ I_n) = 0 \quad (10)$$

@ indicates the bialternate product while I_n is the n-square identity matrix. Hopf bifurcations cause limit cycles and should be eliminated because limit cycles make optimization and control tasks very difficult. More details can be found in Kuznetsov [21] and Govaerts [22] respectively.

2.2.2. Optimal Control

Pyomo.dae, as referenced by Hart, et al. [24] is used for optimal control calculations. Pyomo.DAE extends the Pyomo optimization framework, making it suitable for solving dynamic systems of differential and algebraic equations. It provides a symbolic environment for addressing differential-algebraic equation systems within

optimization problems. This capability is crucial in process systems engineering, chemical kinetics, and control systems, where understanding the dynamic response of systems is essential.

At its core, Pyomo.DAE enables users to define time-varying variables, derivatives, and constraints symbolically, which can be easily integrated into a Pyomo model. Users can define continuous sets for time or other variables, which can be used to specify derivatives over those sets. This symbolic approach allows users to discretize continuous differential-algebraic equation systems using finite difference, collocation, or orthogonal collocation methods, transforming continuous differential equations into algebraic equations solvable with standard solvers. The framework handles both initial-value problems and dynamic optimization problems. In dynamic optimization, Pyomo.DAE facilitates the formulation of time-dependent objective functions and constraints, making it particularly useful in optimal control, energy systems, and chemical process scheduling problems.

One of the major advantages of Pyomo.DAE is that it is compatible with the Pyomo ecosystem. This allows users to leverage existing solver interfaces, variable bounds, nonlinear constraints, and objective functions within a combined static and dynamic modeling framework. Furthermore, the symbolic framework makes it easier to perform model verification, automatic differentiation, and sensitivity analysis. Pyomo.DAE provides a flexible, extensible, and open-source environment for modeling, simulation, and optimization of dynamic systems. By integrating symbolic modeling of DAEs with powerful discretization and optimization capabilities, it offers a unique framework for solving complex time-dependent problems. Its tight integration with Pyomo enables the efficient solution of both simple and complex dynamic optimization problems, making it a cornerstone of modern computational modeling of dynamic systems. In Pyomo.DAE, the differential equations are converted to a nonlinear program (NLP) using the orthogonal collocation method. The NLP is solved using IPOPT [25].

2.3. Formation of Stability Dataset from MATCONT results

A stability dataset was developed based on the results from numerical continuation calculations carried out in MATCONT. The stability dataset consists of rows, each representing a continuation point from an equilibrium branch. The columns in each row consist of the state variables, the bifurcation parameter, and a stability measure. The stability measure is a numerical value derived from the Jacobian matrix. The Jacobian matrix is computed numerically at each equilibrium point. The eigenvalues are then computed automatically using MATLAB. The maximum value of the real part of these eigenvalues is then computed as a scalar stability measure.

The stability measure is computed using "eig_real_max = max(real(eigvals))" in MATLAB. The stability measure is a quantitative metric in which negative values indicate locally asymptotically stable equilibria, positive values indicate instability, and a zero crossing indicates a Hopf bifurcation. The stability dataset is then saved as a CSV file. The dataset can then be used in subsequent computational calculations to perform classification or regression to identify stability boundaries or approximate bifurcations.

2.4. Neural Network Surrogate for Stability Prediction

Direct embedding of eigenvalue calculations into IPOPT-based optimal control is impractical for several reasons: (i) computing eigenvalues at each time step is computationally expensive; (ii) the mapping from states to the maximum eigenvalue is non-smooth near eigenvalue crossings; and (iii) symbolic differentiation of eigenvalues is challenging.

Prior to neural network training, all input variables were standardized to improve numerical conditioning and training stability. Let x_{raw} denote the vector of state variables and bifurcation parameter obtained from the stability dataset. For each input variable j, the training mean μ_j and training standard deviation σ_j were computed over the training dataset as the arithmetic mean and standard deviation, respectively. The training mean for input variable j is defined as the arithmetic average over all training samples as $\mu_j = \frac{1}{N}\sum_{k=1}^{N} x_j^{(k)}$, and the training standard deviation for the input variable $j$is defined as: $\sigma_j = \frac{1}{N}(\sum_{k=1}^{N} x_j^{(k)} - \mu_j)^2$.

The standardized inputs were defined as:

$$x_j = \frac{x_{\text{raw},j} - \mu_j}{\sigma_j} \qquad (11)$$

This transformation ensures that each input variable has zero mean and unit variance over the training set, thereby improving neural network conditioning and gradient-based optimization performance.

The vectors μ, σ μ and σ computed during training were stored and embedded identically within the Pyomo optimal control formulation to ensure consistency between neural network training and deployment.

To overcome these limitations, a feedforward neural network is trained to approximate the maximum eigenvalue as a smooth function of the system state and bifurcation parameter. A typical architecture employs the hyperbolic tangent (tanh) as a smooth activation function. If the input vector is denoted by x, which are the scaled variables, then the network is defined as:

$$\begin{aligned} z1 &= tanh(W1\,x + b1) \\ z2 &= tanh(W2\,z1 + b2) \\ \lambda\_max\_NN &= W3\,z2 + b3 \end{aligned} \qquad (12)$$

Because tanh is infinitely differentiable, the network is fully smooth, guaranteeing the availability of first and second derivatives required by IPOPT. Here, W1, W2, and W3 are the weights that scale and combine inputs or hidden-layer features, while b1, b2, and b3 are the biases that allow neurons to shift their activation independently of inputs. Without biases, the network output would be constrained to pass through the origin, limiting flexibility.

The hidden-layer outputs z1, z2 represent nonlinear combinations of the inputs and previous-layer features, respectively. Each element of z_1 is a smoothed combination of the original inputs, while each element of z2 encodes more abstract patterns extracted from z1. The final output λ_max_NN provides a smooth approximation of the maximum real eigenvalue, enabling efficient and differentiable stability evaluation within the optimal control problem. Figure 1 shows a chart describing the computational strategy.

The integration into optimal control is done using a soft penalty formulation where we use a smooth_max function that converts λ into a smooth, nonnegative penalty that only "activates" when the system is unstable.

$$s_{\max}(\lambda+\varepsilon_1) = smooth - \max(\lambda+\varepsilon_1) = \frac{(\lambda+\varepsilon_1)+\sqrt{(\lambda+\varepsilon_1)^2+\varepsilon_1}}{2} \quad (13)$$

λ is the neural network's predicted maximum eigenvalue at the current state and parameters, while ε is a small positive safety margin to ensure differentiability. The soft penalty formulation involves the new objective function, where the original objective function $optv(t) = (\sum(x(t))^2 + (y(t))^2$ is modified to $\sum(optv(t) + \alpha_{hopf}.s1^2{}_{max}$ α_{Hopf} control how aggressively instability is penalized and ε_1 preventing numerical issues at exactly λ = 0 and slightly shifting the stability boundary.

3. Results and Discussion

The bifurcation analysis revealed a Hopf bifurcation at (x,y, N, K) values of (0.097074, -0.852819, 0.308588, 0.918032). This is shown in Figure 1a. The limit cycle resulting from this Hopf bifurcation is seen in Figure 1b.

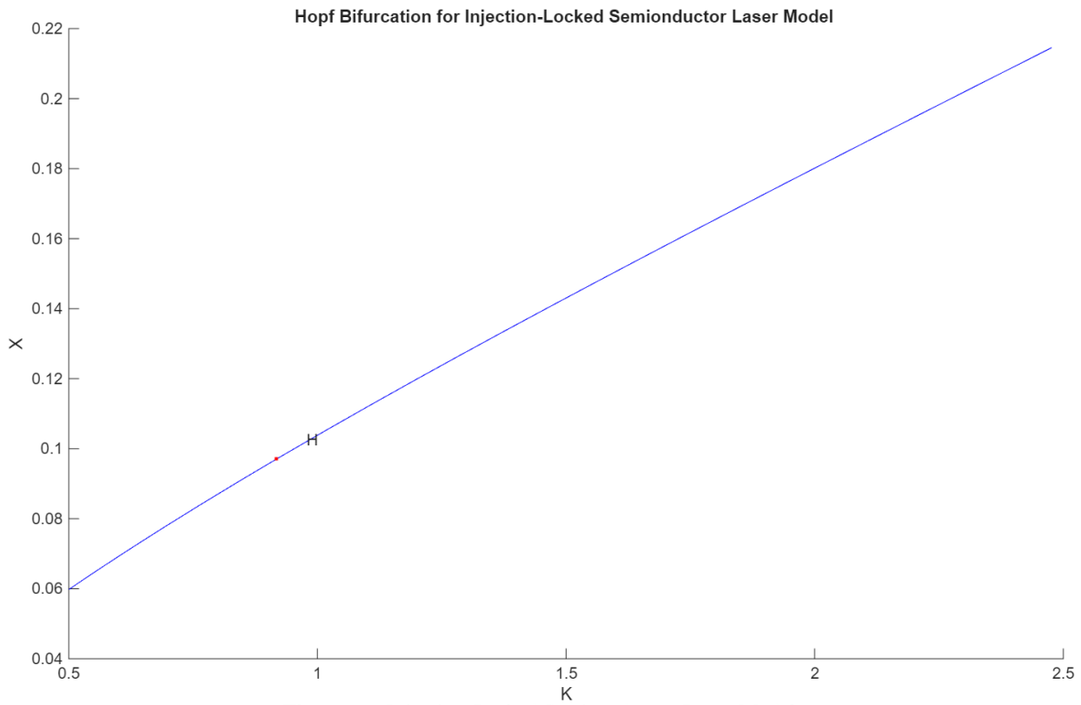

Figure 1a. Injection-Locked Semiconductor Laser Model.

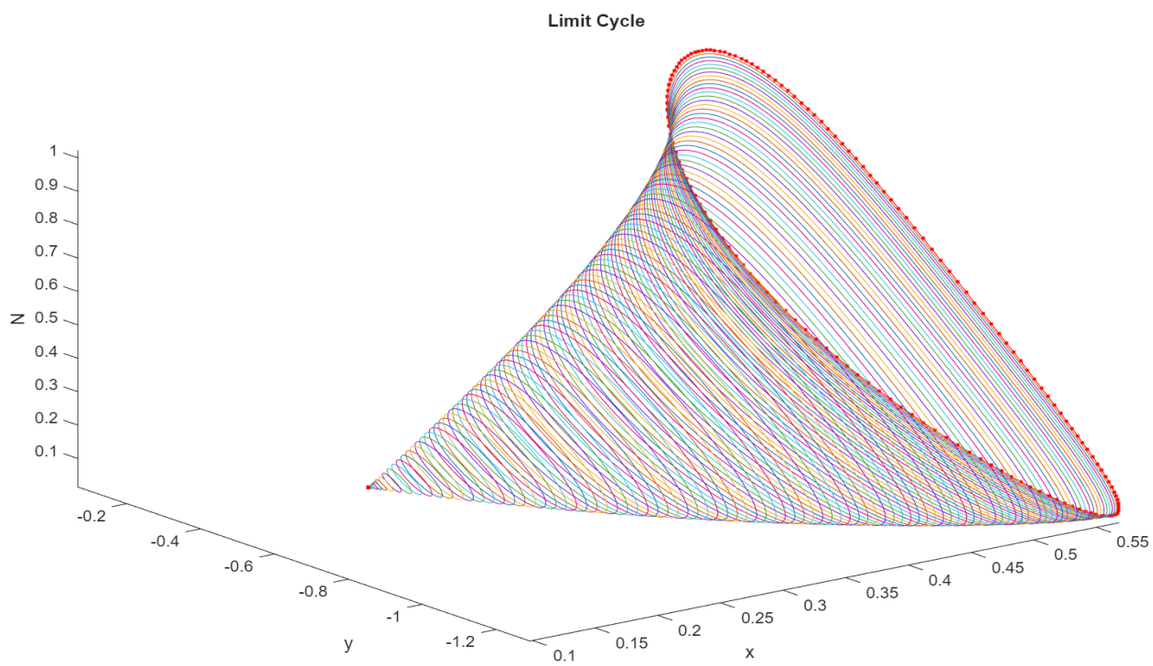

Figure 1b. Limit Cycle for Injection-Locked Semiconductor Laser Model.

For the optimal control, when no measures are taken, $(\sum optv(t))^2$is minimized, and when the soft penalty formulation is integrated, $\sum(optv(t)+\alpha_{hopf}.s_{\max}(\lambda+\varepsilon_1))^2$ is minimized. When no measures were taken, the obtained value of $(\sum optv(t))$ was 77.727, and when the soft penalty formulation is integrated, with $\alpha_{hopf} = 0.25$; The obtained value of $(\sum optv(t))$ was 58.581.

A more beneficial solution is obtained by avoiding the limit cycle that causes Hopf bifurcations. Figures 2a, 2b, 2c, and 2d show various Hopf bifurcation profiles. Comparing plots 2b and 2d reveals that the Hopf constraint results in a k profile without significant oscillations.

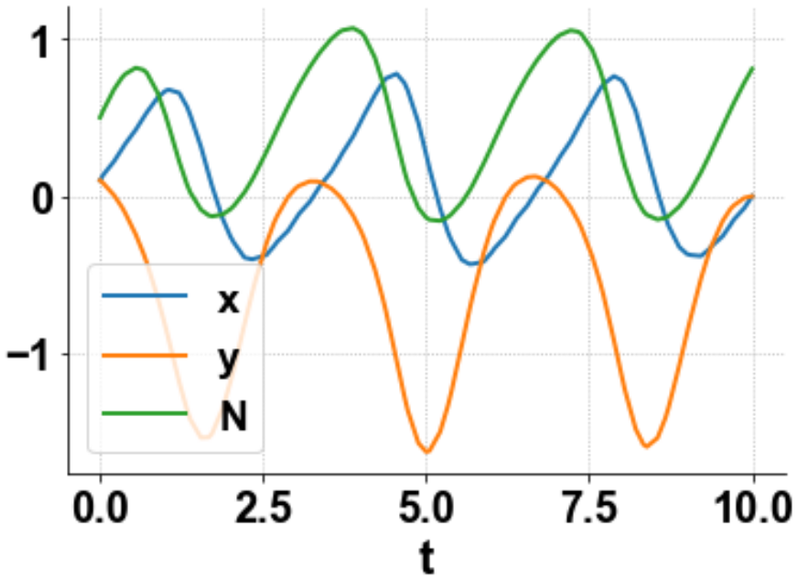

Figure 2a. x, y, N profiles no Hopf constraint.

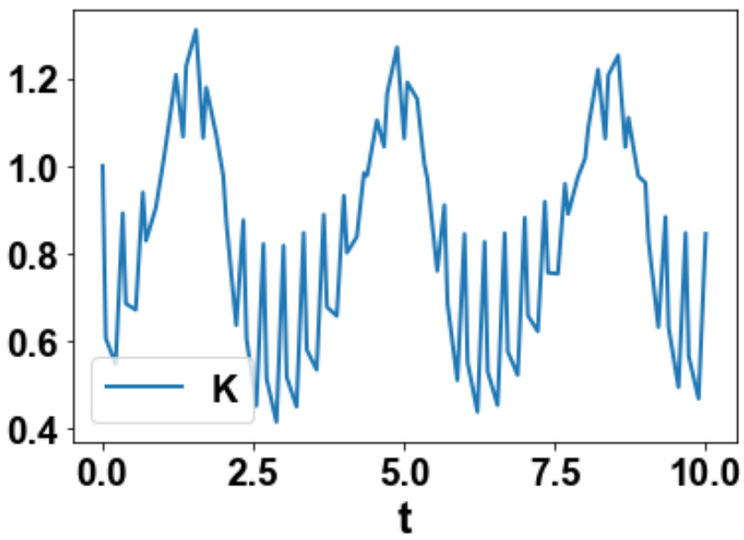

Figure 2b. K profile no Hopf constraint.

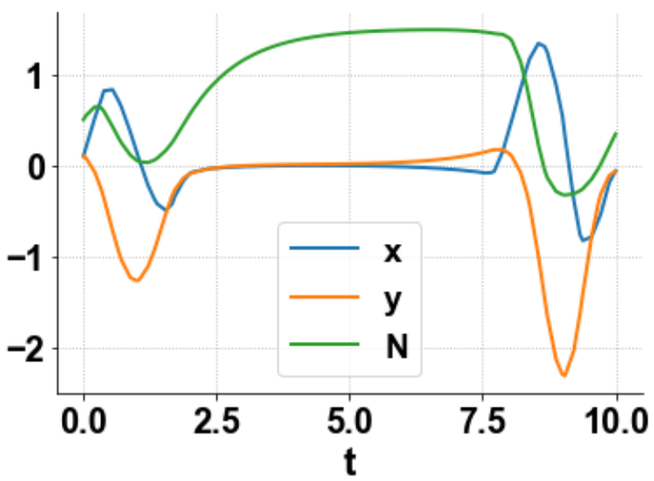

Figure 2c. x, y, N profiles with Hopf constraint.

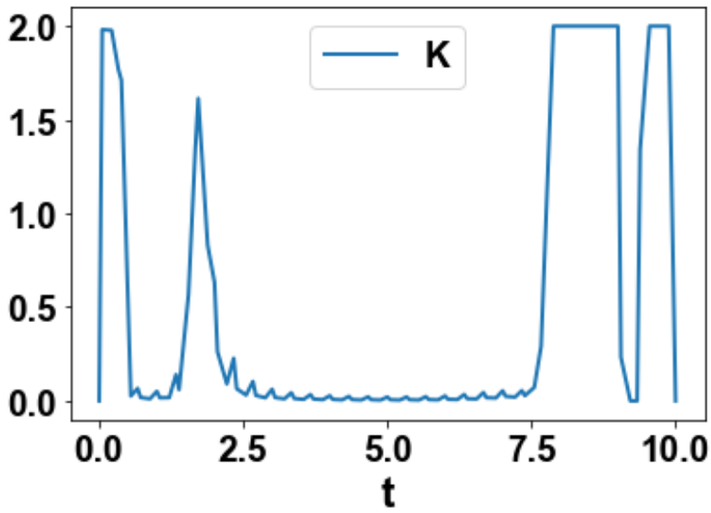

Figure 2d. K profile with Hopf constraint.

The results obtained through this research clearly indicate that the Hopf bifurcation is an important phenomenon influencing the dynamical behavior of injection-locked semiconductor lasers. They also demonstrate the effectiveness of the proposed optimal control mechanism in suppressing undesirable oscillations. The bifurcation analysis using the MATCONT tool showed that a Hopf bifurcation occurs at specific values of the state variables and injection, indicating a transition from stability to oscillation in the system. As seen in Figure 1b, the existence of the limit cycle aligns with theoretical expectations.

From a control perspective, the presence of a Hopf bifurcation is highly detrimental, as it indicates oscillatory dynamics that may negatively affect laser operation. A comparison of the uncontrolled and controlled versions clearly shows the usefulness of adding the soft constraint concerning Hopf bifurcations in terms of the optimality criteria. The first case shows that without the stability constraint, the optimization algorithm finds a minimum of the objective function; however, it does so in the region of instability, where a higher value (77.727) is obtained compared to the second scenario. With the inclusion of the soft penalty formula, we see a substantially lower value (58.581), indicating that the system's performance improves while maintaining stability.

One of the critical findings is the neural network's ability to represent the stability constraint, enabling us to implement it effectively in an optimization task. Instead of performing time-consuming computations based on eigenvalue analysis, we have found a smooth, differentiable representation of the stability boundary, allowing us to apply the gradient-based solver IPOPT.

The variations demonstrated in Figure 2b and Figure 2d also demonstrate the influence of the Hopf constraint on the control input signal. In the absence of the constraint, the injection strength profile oscillates, indicating that the system operates near an unstable regime. However, thanks to the Hopf constraint, the control input profile is much smoother, indicating the system operates in a stable regime, avoiding bifurcation points.

In conclusion, one may claim that the proposed algorithm is indeed a robust tool for controlling systems exhibiting nonlinear behavior and suffering from bifurcation-induced instability. Such an approach is efficient and computationally feasible and can be used for controlling any other similar engineering system.

4. Conclusions

In this paper, a systematic methodology was introduced for investigating the dynamics and optimal stabilization of the nonlinear injection-locked semiconductor laser system. After developing the nondimensionalized mathematical model, the complex interaction of the optical field and the carrier density was considered and analyzed. Applying the MATCONT algorithm to the system, Hopf bifurcation points were identified as the onset of limit-cycle behavior.

To address the problem, an optimal control problem was formulated in this work using Pyomo.DAE modeling language with an approximation of the system stability boundary via neural networks as a substitute for eigenvalue computation. This methodology avoids computational inefficiency due to eigenvalues while preserving smoothness for efficient optimization. Additionally, the use of a soft penalty constraint helps avoid unstable zones.

Based on the conducted simulations, the effectiveness of the proposed method was validated. Specifically, the absence of oscillations in the response and the minimization of the objective functions were observed as a result of introducing proper controls. In summary, this study has demonstrated how bifurcation analysis, machine learning models, and optimal control can all be used in one study.

References

[1] R. Lang, "Injection locking properties of a semiconductor laser," *IEEE Journal of Quantum Electronics*, vol. 18, no. 6, pp. 976-983, 1982. https://doi.org/10.1109/JQE.1982.1071632

[2] G. P. Agrawal and N. K. Dutta, *Semiconductor lasers*. New York: Van Nostrand Reinhold, 1993.

[3] L. A. Coldren, S. W. Corzine, and M. L. Mashanovitch, *Diode lasers and photonic integrated circuits*. Hoboken, NJ: Wiley, 2012.

[4] B. Krauskopf and S. Wieczorek, *Bifurcations in laser systems*. Amsterdam, Netherlands: Elsevier, 2002.

[5] S. Wieczorek, B. Krauskopf, T. B. Simpson, and D. Lenstra, "The dynamical complexity of optically injected semiconductor lasers," *Physics Reports*, vol. 416, no. 1-2, pp. 1-128, 2005. https://doi.org/10.1016/j.physrep.2005.06.003

[6] T. Erneux and P. Glorieux, *Laser dynamics*. Cambridge, UK: Cambridge University Press, 2010.

[7] F. Gustave, L. Columbo, G. Tissoni, M. Brambilla, F. Prati, and S. Barland, "Phase solitons and domain dynamics in an optically injected semiconductor laser," *Physical Review A*, vol. 93, no. 6, p. 063824, 2016. https://doi.org/10.1103/PhysRevA.93.063824

[8] B. Garbin, M. Marconi, J. Javaloyes, S. Barland, and M. Giudici, "Experimental evidence of phase solitons in semiconductor lasers," *Nature Communications*, vol. 8, p. 14881, 2017.

[9] S. Terrien, B. Krauskopf, and N. G. R. Broderick, "Bifurcation analysis of the Yamada model for a pulsing semiconductor laser with saturable absorber and delayed optical feedback," *SIAM Journal on Applied Dynamical Systems*, vol. 16, no. 2, pp. 771-801, 2017. https://doi.org/10.1137/16M1099236

[10] M. S. Torre and C. Masoller, "Exploiting nonlinear dynamics of optically injected semiconductor lasers for sensing," *Photonics*, vol. 6, no. 2, p. 45, 2019. https://doi.org/10.3390/photonics6020045

[11] M. Virte, M. Sciamanna, K. Panajotov, and H. Thienpont, "Chaos and nonlinear dynamics in semiconductor lasers for secure communications," *Nature Photonics*, vol. 13, no. 1, pp. 23–31, 2019.

[12] J. Robertson, M. Hejda, J.-P. Goedgebuer, L. Larger, and I. Fischer, "Neuromorphic photonics with semiconductor lasers," *Journal of Lightwave Technology*, vol. 38, no. 2, pp. 309–317, 2020.

[13] M. C. Soriano, D. Brunner, M. A. Escalona-Morán, C. R. Mirasso, and I. Fischer, "Delay-based photonic reservoir computing," *Reviews of Modern Physics*, vol. 93, no. 1, p. 011006, 2021.

[14] J. Mørk, L. F. Lester, and A. C. Tropper, "Semiconductor lasers for photonic computing," *Nature Reviews Physics*, vol. 3, no. 10, pp. 705–722, 2021.

[15] X. Li, Y. Wang, J. Chen, H. Liu, and Q. Zhang, "Nonlinear dynamics and bifurcation control in semiconductor lasers with optical injection," *Optics Express*, vol. 30, no. 18, pp. 32645–32660, 2022.

[16] Y. Wang, J. Li, H. Zhang, M. Liu, and Y. Chen, "Dynamical regimes of injection-locked semiconductor lasers," *IEEE Journal of Quantum Electronics*, vol. 58, no. 3, pp. 1–9, 2022.

[17] G. Liu, Y. Shen, R. Li, J. Yu, X. He, and C. Wang, "Optical ReLU-like activation using injection-locked semiconductor laser," *Optics Letters*, vol. 48, no. 5, pp. 1123–1126, 2023.

[18] T. Heil, C. Otto, M. Peil, and W. Elsäßer, "Nonlinear dynamics of semiconductor lasers with feedback and injection," *Physical Review A*, vol. 107, no. 2, p. 023501, 2023.

[19] Z. Zhang, H. Li, Y. Wang, X. Chen, and Q. Liu, "Bifurcation control in semiconductor laser systems," *Chaos: An Interdisciplinary Journal of Nonlinear Science*, vol. 33, no. 4, p. 043125, 2023.

[20] Y. Shen, J. Li, H. Wang, X. Chen, and Z. Liu, "Photonic neural networks using injection-locked lasers. ," *Nature Communications*, vol. 15, p. 2143, 2024.

[21] Y. A. Kuznetsov, *Elements of applied bifurcation theory*. New York: Springer, 1998.

[22] W. J. F. Govaerts, *Numerical methods for bifurcations of dynamical equilibria*. Philadelphia, PA: SIAM, 2000.

[23] A. Dhooge, W. Govaerts, and Y. A. Kuznetsov, "MATCONT: A MATLAB package for numerical bifurcation analysis of ODEs," *ACM Transactions on Mathematical Software*, vol. 29, no. 2, pp. 141-164, 2003. https://doi.org/10.1145/779359.779362

[24] W. E. Hart *et al.*, *Pyomo – optimization modeling in Python*. Cham, Switzerland: Springer, 2017.

[25] A. Wächter and L. T. Biegler, "On the implementation of an interior-point filter line-search algorithm for large-scale nonlinear programming," *Mathematical Programming*, vol. 106, pp. 25-57, 2006. https://doi.org/10.1007/s10107-004-0559-y

[26] A. Dhooge, W. Govaerts, Y. A. Kuznetsov, W. Mestrom, and A. Riet, *MATCONT: A continuation toolbox in MATLAB*. Ghent, Belgium: University of Ghent, 2004.